Brownian Motion and Quantum Dynamics of Magnetic Monopoles in Spin Ice: Supplementary Information

L. Bovo[1], J. A. Bloxsom[1], D. Prabhakaran[2], G. Aeppli[1], S. T. Bramwell[1].

1. London Centre for Nanotechnology and Department of Physics and Astronomy, University College London, 17-19 Gordon Street, London, WC1H OAH, U.K.

2. Department of Physics, Clarendon Laboratory, University of Oxford, Park Road, Oxford, OX1 3PU, U.K.

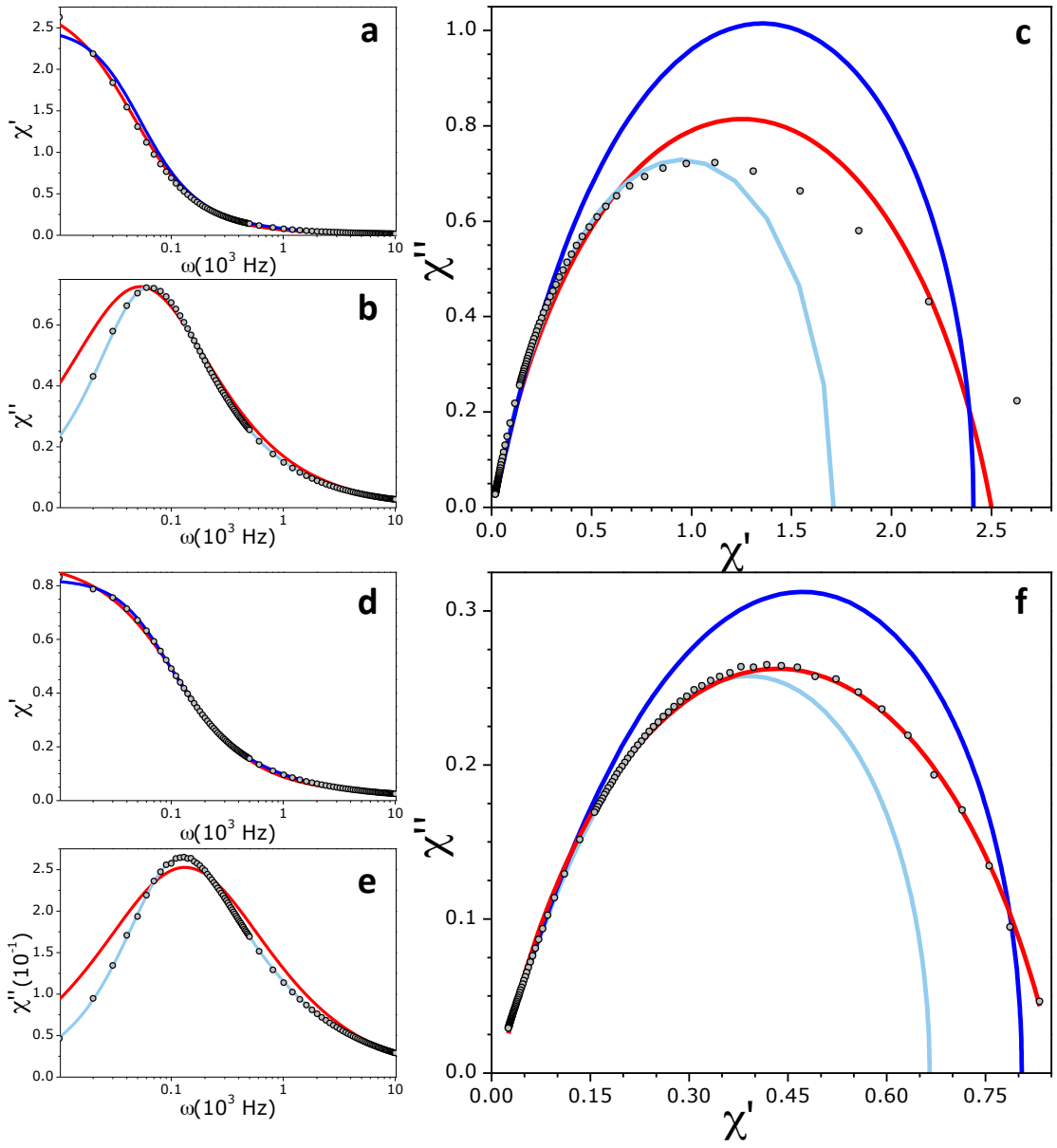

Supplementary Figure S1: **Comparison between Cole-Cole (CC) and Cole-Davidson (CD) model.** Data taken at zero dc-field and $T = 1.95$ K: **(a)** real and **(b)** imaginary susceptibility and **(c)** argand diagram. Data taken at zero dc-field and $T = 6$ K: **(d)** real and **(e)** imaginary susceptibility and **(f)** argand diagram. CC model: The red line fits all the data with the same set of four parameters: χ_T, χ_S, α and τ, as defined in the main text. The deviation that happen at low temperature and low frequency is discussed in the text. CD model: The blue and turquoise lines represent the two best fit obtained analysing experimental data. It must be noted that, unlike the CC model, there is not a unique set of parameters that can fit simultaneously the three diagrams.

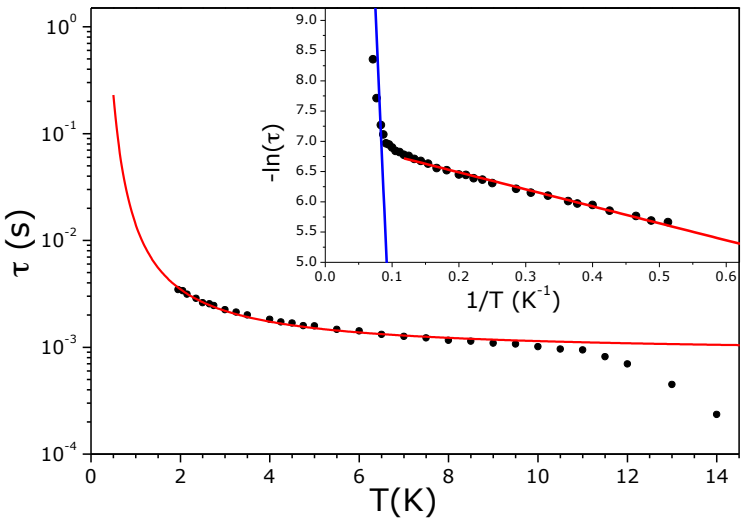

Supplementary Figure S2: **Temperature dependence of relaxation time.** Experimental data extrapolated from the CC-fitting (black circles). The red line is a fit to the free diffusion of topological defects in the nearest neighbour approximation[20]. Inset: same data shown on a different scale. The blue line represents the fit to an Arrhenius law, with an activation energy of about 250 K, compatible with a classical Orbach-like mechanism (main text).

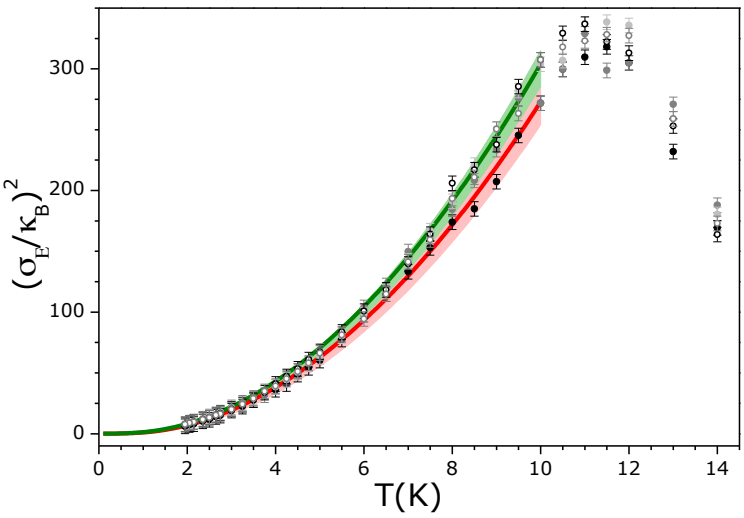

Supplementary Figure S3: **Variance of the effective energy activation barrier versus temperature.** Temperature dependence of the experimental variance in energy scale as a function of weak applied field $0 \leq \mu_0 H \leq 0.05$ T (circles, same colour code is maintained as in Fig. 3). Error bars represent the standard deviation. Red and green indicate, respectively, applied fields of $\mu_0 H = 0$ and the set of finite fields. The line is Eqn. S3 with $\sigma_{1,2} = 0.84(1), 3.40(5)$ respectively in zero field and $1.15(1), 3.40(5)$ in finite field (Fig. 4). The shading indicates the maximum possible systematic error (absolute minima and maxima) in the monopole density. The deviation at $T > 10$ K is related to a change in relaxation mechanism (main text).

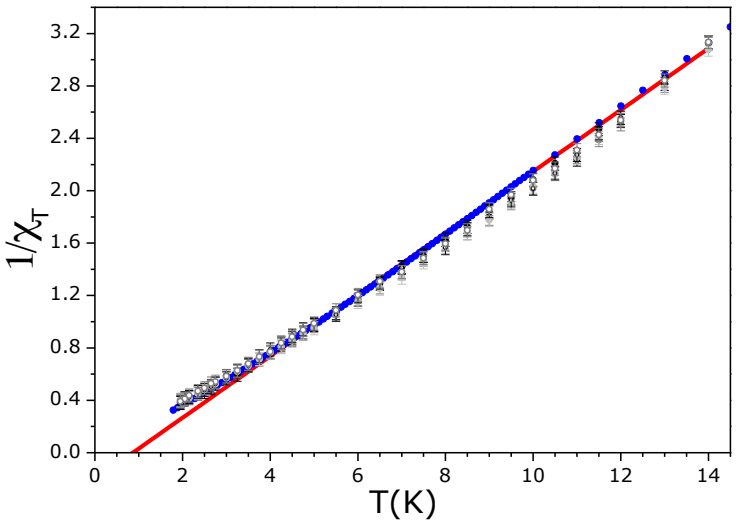

Supplementary Figure S4: **Isothermal susceptibility.** Results obtained fitting experimental data in the limit of weak applied field ($0 \leq \mu_0 H \leq 0.05$ T); the same colour code is maintained, as in the main paper. Error bars represent the standard deviation. The blue circles represent the bulk SQUID magnetometry measurement. The red line is the fit to a Curie-Weiss behaviour as reported in the text.

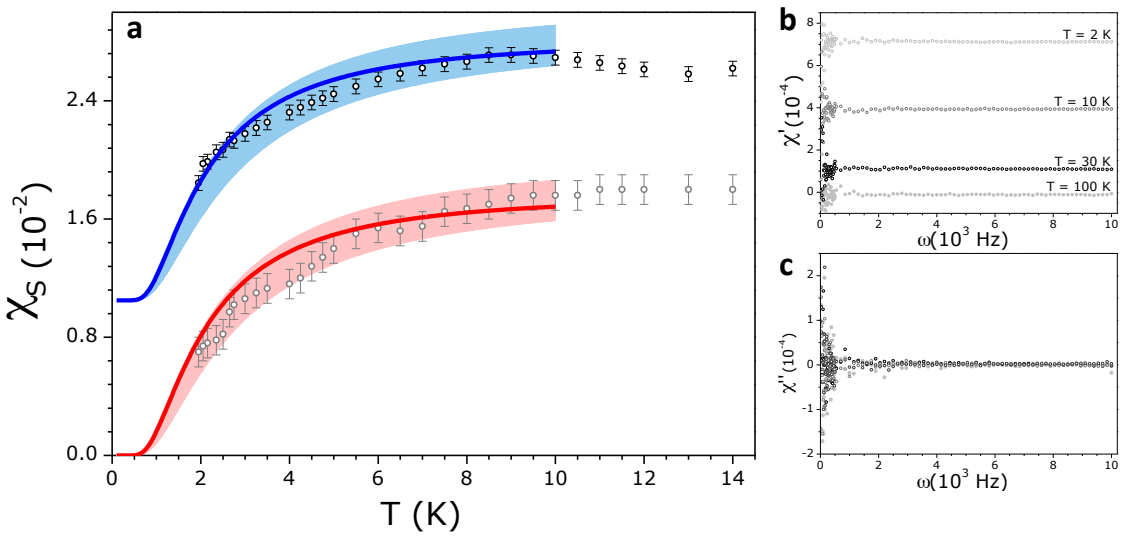

Supplementary Figure S5: **Experimental adiabatic susceptibility.** **(a)**: (grey circles) extrapolated from CC-fitting and (black circles) the measured value of $\chi'(10^4\ \mathrm{s}^{-1})$. The red line represent the expected monopole density adjusted by a scale factor; the shaded area indicates the maximum systematic error (absolute minima and maxima) in the estimated monopole density (main text and Figs. 4 and 5). The blue line, and respective shadow, is obtained simply by shifting the red line of an offset of about 0.0105(1). Error bars represent the standard deviation. The shading indicates the maximum possible systematic error (absolute minima and maxima) in the monopole density. **Instrumental response**: Real **(b)** and imaginary **(c)** component of the susceptibility measured at different temperatures for a single crystal of $LiYF_4$: 0.3 *at.* % Ho; the signal is at least two orders of magnitude lower than in the case of the spin-ice crystal in the entire temperature range.

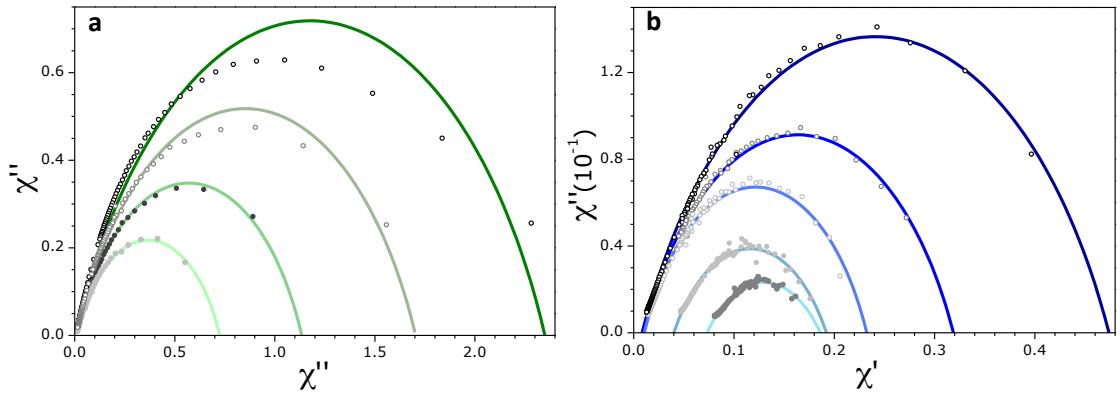

Supplementary Figure S6: **Cole-Cole plot and respective CC-fit of data taken at $\mathbf{T = 1.95}$ K at different applied field. (a)**: representative data taken at, from dark to light green, $\mu_0 H$ of 0.1, 0.2, 0.3 and 0.4 T, respectively. **(b)**: representative data taken at, from dark blue to turquoise, $\mu_0 H$ of 0.5, 0.7, 0.8, 0.9 and 1 T, respectively.

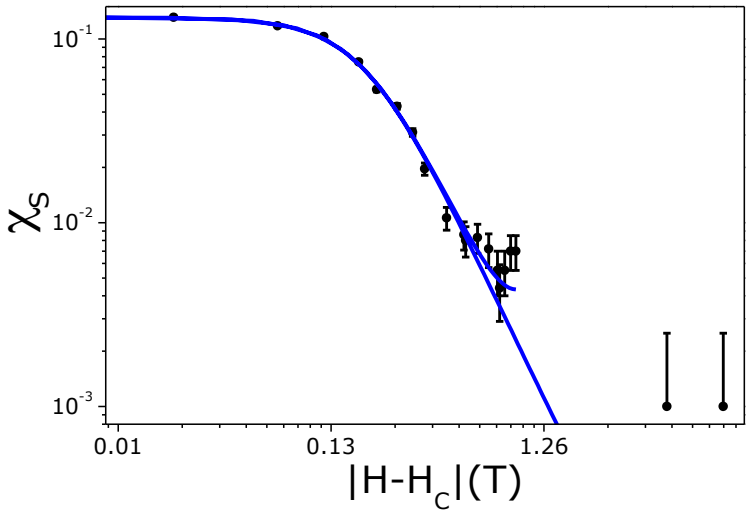

Supplementary Figure S7: **Adiabatic susceptibility versus applied field, Log-Log plot.** Experimental χ_{S} extrapolated from data at $T = 1.95$ K. Error bars represent the standard deviation. The blue line shows that the observed exponent of $\alpha = 2$ for $\chi_{\mathrm{S}} \sim |H - H_{\mathrm{C}}|^{(-\alpha)}$.

Supplementary Note 1

Specific Heat

The specific heat of single crystal $Dy_2Ti_2O_7$ was measured with a Quantum Design Physical Properties Measurement (PPMS) System. The Debye-Hückel theory of Ref.[26], along with a correction for double charge monopoles (Bloxsom, J. A. unpublished) was used to fit the specific heat data over the entire range of measured temperature, and so to extract the monopole charge density as a function of temperature. The monopole chemical potential was used as a fitting parameter and was refined to be ~ 4.33 K, which is in good agreement with theory[26]. The Debye-Hückel theory is accurate only for small x/T. This means that it is accurate at low temperature, and also a reasonable approximation at high temperature, but breaks down at intermediate temperature, near to the peak in the specific heat at ~ 1 K. Although this leads to a significant systematic error on the specific heat, the error that propagates through to $x(T)$ is relatively small. Estimates of this systematic error were made by altering parameters in the partition function within reasonable bounds, to give the envelope of curves exhibited in the paper. The estimated $x(T)$ was found to be in close agreement with that derived from numerical simulations (Kaiser, V. private communication) and is clearly sufficiently accurate for our purpose. Full details of the specific heat analysis will be published separately.

Supplementary Note 2

Model Used to Fit the data

In the main text we note that the relaxation time τ does not have the same physical interpretation as that arising in conventional models of paramagnetic spin relaxation. However this fact may be neglected for fitting purposes, and the data analysis reduces to a familiar problem of fitting $\chi(\omega)$ to conventional phenomenological forms.

The Debye model, with a single exponential relaxation of the susceptibility fails in the description of experimental data. Various empirical equations have been formulated to give the variation of $\mathrm{Im}[\chi(\omega)] = \chi''$ with $\mathrm{Re}[\chi(\omega)] = \chi'$ as the frequency is varied, taking into account the presence of different distributions of relaxation times. In particular, as discussed in the main text, we tested two of the most commonly used models: the Cole-Cole (CC)[34] and Cole-Davidson (CD)[56] formalisms. Supplementary Figure S1 shows an illustrative comparison between the two representations. The CC formalism works rather well in all range of frequency for a wide interval of temperature, 3.5 K $\leq T \leq$ 14 K. At low temperatures, in the low frequency regime, the experimental data start to deviate from the model, showing an increasing asymmetry.

Nevertheless, it is possible to fit all data with the same set of four parameters for each temperature (red lines in Supplementary Figure S1 show two examples for data taken at $T = 1.95$ K and 6 K, respectively). On the contrary, when the CD-model is applied, the fit to the experimental data is poorer, as shown in Supplementary Figure S1. In particular, it is not possible to find a unique set of parameters to simultaneously fit the frequency dependence of the real and imaginary susceptibility as well as the argand diagram ($\chi''_{\mathrm{T}} = f(\chi'_{\mathrm{T}})$). It is clear then that the CC formalism seems to give a more representative picture of the dynamics in $Dy_2Ti_2O_7$. This seems physically reasonable as the CC model assumes a distribution of logarithmic relaxation times that is cut off exponentially at high frequency, while the DC model assumes a power law to high frequency. The latter is not consistent with what is known about the magnetic dynamics in spin ice, where the monopole hop rate would presumably

lead to a cut-off at high frequency. Hence the superior performance of the CC model is plausible. Undoubtedly, the determination of the proper distribution of relaxation times for a spin-ice system could in principle lead to a better interpretation of experimental data, especially of the asymmetry showed at low temperatures in the low frequency regime.

Supplementary Note 3

Relaxation Time

The magnetic relaxation time as a function of temperature of $Dy_2Ti_2O_7$ is displayed in Supplementary Figure S2. The general dynamic behaviour, in good agreement with previous experimental data[22], is consistent with the presence of two different regimes. At enough high temperature, above 10 K, the time scale drops dramatically due to a thermally activated process (Orbach-like mechanism) with an energy barrier of few hundreds kelvin compatible with higher energy crystal field levels being populated. This barrier, $E_a \approx 250$ K, is insurmountable below 10 K, and the system enters a quasi-plateau region. A further lowering of the temperature, below 2 K - outside the temperature range investigated in this work - would have caused a sharp upturn of the relaxation time[22]. Following the work done by Jaubert and Holdsworth[20], it is possible to interpret the quasi-plateau region with the presence of a thermal assisted quantum tunnelling through the crystal field barrier: below 10 K the spins are Ising like and the system can be represented by stochastic single spin dynamics, or in 'monopole' language by the creation and diffusion of the topological defects.

In a first approximation[20], it is possible to consider an Arrhenius law of the type:

$$\tau = \tau_0 \exp(2J_{\text{eff}}/kT), \tag{S1}$$

where τ_0 is the microscopic tunnelling time and $2J_{\text{eff}}$ is the energy cost of a single free topological defect in the nearest neighbour approximation and is half of that of a single spin flip. The red line in Supplementary Figure S2 represents the best fit to Eqn. S1

with $\tau_0 = 8.6(2) \times 10^{-4}$ s and $2J_{\rm eff}/k = 2.8(1)$ K, in close agreement with the results of Jaubert and Holdsworth[20] and in line with the analysis and description that we have proposed in the main paper. This expression has been proven[20] to work rather well in the semi-plateau regime, but it starts to fail below 2 K underestimating the relaxation time at very low temperature. Nevertheless, they showed[20] how it is possible to interpret the magnetic relaxation of $Dy_2Ti_2O_7$, in the whole temperature range in terms of the diffusive motion of monopoles in the canonical ensemble, constrained by a network of 'Dirac strings' filling the quasi-particle vacuum.

A similar way to rephrase the problem is to consider that at any given temperature there is only a well defined fraction x of flippable spins (or density of monopoles, reverting to the topological defects representation) that can directly contribute to the magnetic relaxation process. Spins that are not associated with monopoles can flip at much hinger cost and cannot contribute to the dynamics. In this work, indeed we have shown that once taken into account the thermal evolution of the density of monopoles and the temperature factor characteristic of a diffusive (Brownian) motion (main text), the resulting characteristic hopping rate turns out to be temperature independent, symptomatic of a spin relaxation that occurs by quantum tunnelling.

Supplementary Note 4

Ambiguities in the Interpretation of the Dispersion of Relaxation Times

It should be noted that Eqn. 4 of the main text is only strictly valid for $h_1, h_2 \ll 1$ which is marginal for the data considered here. Unfortunately the inversion of a logarithmic time distribution to a frequency distribution is an ill defined mathematical problem[37] that can only be accomplished in a satisfactory way for narrow distributions. This means that our simple model is not ruled out, but nor is it unambiguously implied by our data. In contrast, as shown in Ref.[37], within the Cole-Cole model, the variance of effective energy barriers $\sigma_{\rm E}^2$

may be extracted from the relationship:

$$\sigma^2_{\ln\tau} = \frac{\sigma^2_{\mathrm{E}}}{k^2T^2}. \tag{S2}$$

Thus our experimental result may be cast into the form:

$$\sigma^2_{\mathrm{E}} = (kT)^2(\sigma_1^2 + x\sigma_2^2), \tag{S3}$$

where σ_1, σ_2 now become uninterpreted (but still temperature-independent) parameters. This quantity is plotted in Supplementary Figure S3.

While Eqn. S3 is weaker than Eqn. 4 (main text) at the level of physical interpretation, the presence of factors of kT in its right hand side clearly imply a quantum relaxation and its factor of x implies cooperative dynamics involving magnetic monopoles. The direct field interaction that we have suggested is one plausible explanation of this.

A minimal conclusion that may be drawn from our analysis is as follows. Assuming the monopole model, we can directly measure the diffusion constant $D(T)$. However, this argument cannot be reversed, so the behaviour of the measured relaxation time using the Cole-Cole model does not in itself infer the role of magnetic monopoles. This ambiguity may be traced to the fact that the relaxation due to monopoles takes the form of an effective spin relaxation (see above). In contrast, the fact that the dispersion of the logarithmic relaxation time correlates with the measured monopole density does directly implicate magnetic monopoles in the relaxation process.

Supplementary Note 5

Isothermal Susceptibility

For the sake of completeness, Supplementary Figure S4 reports the evolution of isothermal susceptibility as a function of temperature in the limit of weak applied field ($\mu_0 H \leq 0.05$

T). For comparison, the bulk magnetometry SQUID data (blue circles) of the same sample are also displayed in Supplementary Figure S4. The best fit (red line) to an apparent Curie-Weiss law $\chi_{\rm T} = C'/(T-\theta)$ gives rise to a Curie Constant $C' = 4.25(5)$ K and $\theta = 0.8(1)$ K. The experimental data deviate from this fitting at low temperature. Similar behaviour was reported for another spin ice compound[38,57]. There it was found that the Curie-Weiss law is only apparent for spin ice materials and simply approximates a Curie Law crossover from $\chi_{\rm T} = 2C/T$ at low temperature, to $\chi_{\rm T} = C/T$ at high temperature[38]. Here the expected $C = 3.95$ K for $Dy_2Ti_2O_7$. If we write $\chi_{\rm T} = A(T)C/T$ then values of A can be found by transforming the apparent Curie-Weiss law. This gives the values of the pre-factor quoted in the main text.

Supplementary Note 6

Adiabatic Susceptibility

To further assess the consistency of our fits, we tested the reliability of the extrapolation of $\chi'(\omega)$ to the limit of $\omega \to \infty$, to give $\chi_{\rm S}$. First to exclude the possibility of the presence of an apparent background arising from the instrumental response, we determined the latter by measuring a single crystal of paramagnetic $LiYF_4$ doped with 0.3 *at.* % Ho. As shown in Supplementary Figure S5, panels b and c, the signal is at least two orders of magnitude lower than in the case of the spin-ice crystal in the entire frequency and temperature range. Furthermore, as shown in Supplementary Figure S5a, the temperature dependence of the experimental value of χ' for $Dy_2Ti_2O_7$ measured at the highest applied frequency ($\omega = 10^4$ s^{-1}) replicates the temperature dependence of the estimated $\chi_{\rm S}(T)$, showing that $\chi'(\omega)$ tends analytically to the high frequency limit.

As described in the main text, we also measured the ac-susceptibility as a function of an applied static magnetic field along [111]; Supplementary Figure S6 shows argand diagrams obtained at $T = 1.95$ K. First of all, it is worth notice that the deviation in the low frequency

regime of the fitting from the experimental behaviour decreases with the increase of the applied field. Because of the low signal measured at high field, the complete analysis was performed only on data taken at $\mu_0 H < 1$ T; at higher field only the frequency dependence of $\chi'(\omega)$ was fitted. For this reason, we preferred to measure the evolution of $\chi_S(T)$ as a function of temperature at $\mu_0 H = 0.86$ T instead of the actual crossover field where χ_S showed its maximum value (main text and Figures 5 and 6).

Looking at the field dependence of the adiabatic susceptibility, according to mean field theory[30], one would expect $\chi_S \sim |H - H_C|^{(-2/3)}$. Supplementary Figure S7 shows as an example data taken at $T = 1.95$ K. The Log-Log plot clearly indicates an exponent of 2 rather than 2/3.

Supplementary Note 7

Critical Behaviour

If we interpret our field dependent measurements in terms of classical critical exponents, then we are led to the unusual conclusion that the critical point involved is zero dimensional. Thus, if we assume a zero dimensional critical point ($d = 0$) then the scaling laws predict the set of exponents $\delta = -1$, $\gamma = 1$, $\beta = -1/2$ and ν and η are of course undefined. Here we show how these numbers summarise the experimental observations.

In critical point theory we can describe the field and temperature dependence of the order parameter m by 'polar' co-ordinates r, θ, where r is related to the distance from the critical point in the $\{h, t\}$ plane and θ is related to the 'angle' with respect to the t axis. Here $t = T - T_C$, $h = H - H_C$, $m = M - M_C$. The polar equations in their most general form:

$$h \sim r^{\beta\delta} f_h(\theta), \tag{S4}$$

$$t \sim f_t(r, \theta), \tag{S5}$$

$$m \sim r^{\beta} f_m(\theta), \tag{S6}$$

where the three functions $f_{t,m,h}$ on the right hand side are to be determined.

In mean field theory the transformation can be written explicitly:

$$h \sim r^{\beta\delta}\theta(1-\theta^2) \tag{S7}$$

$$t \sim r(1-2\theta^2), \tag{S8}$$

$$m \sim r^{\beta}\theta, \tag{S9}$$

with the set of exponents $\gamma = 1, \beta = 1/2, \delta = 3$.

If we write the equations,

$$h \sim r^{\beta\delta}\tan\theta, \tag{S10}$$

$$t \sim r, \tag{S11}$$

$$m \sim r^{\beta}\theta, \tag{S12}$$

with the exponents $\gamma = 1$, $\beta = -1/2$, $\delta = -1$, we recover our result $\chi = 1/(t+h^2)$. The negative critical exponents look unusual but obey thermodynamics and scaling theory, as is evident from the preceding equations. For example, the Griffiths scaling relation is obeyed: $\gamma = \beta(\delta - 1)$ and m is always an increasing (arctangent) function of h. Applying the usual scaling relations we find: $\alpha = 2$, $d = 0$ and η, ν are undefined as one would expect for a zero dimensional critical point. As the correlation length and its exponent ν are undefined, the dynamical exponent z is also undefined.

Alternatively we could consider a single classical spin in a magnetic field h. It is easy to show that to small h the susceptibility is approximated by $\chi \sim T/(h^2+T^2)$. In this case the polar equations can be satisfied as above, but with $\beta = \delta = 0$; however, the Griffiths scaling relation is not obeyed, suggesting that the classical single spin problem cannot be formally represented as a critical system in the zero temperature limit.

A final possibility is to interpret the exponents in terms of a quantum critical point. Thus,

although the phase transition at zero temperature is first order, at a significant 'distance' away the appropriate renormalisation flow might be dominated by a $T = 0$ critical point of a similar sort to that which occurs the 'transverse field Ising model', but which is in reality removed by the Coulomb interaction, a strongly relevant variable. A quantum critical point typically exhibits the classical critical exponents appropriate to one higher dimension[58]. For a three dimensional system this means that quantum critical points are at the upper critical dimensionality of 4, and so exhibit mean field exponents. As shown above, the observed γ exponent is mean field like, but when combined with the apparent δ exponent of $\delta = -1$ suggests a different universality class. In the theory of quantum critical points[58], this change in dimensionality could be accommodated by a negative dynamical (z) exponent, but this would be physically hard to justify. Thus the field dependent behaviour is distinctly anomalous, however it is viewed.

Supplementary References

56. Davidson, D.W. & Cole R. H. Dielectric Relaxation in Glycerol, Propylene Glycol, and n-Propanol. *J. Phys. Chem.* **19**, 1484 - 1490 (1951).

57. Bramwell, S. T. *et al.* Spin Correlations in $Ho_2Ti_2O_7$: A Dipolar Spin Ice System. *Phys. Rev. Lett.* **87**, 47205 (2001).

58. Hertz, J. A. Quantum Critical Phenomena. *Phys. Rev. B* **14**, 1165 - 1184 (1974).